



HAL
open science

Quantitative proteomic determination of diethylstilbestrol action on prostate cancer

Pierre Bigot, Kevin Mouzat, Souhil Lebdai, Muriel Bahut, Nora Benhabiles, Géraldine Cancel Tassin, Abdel-Rahmène Azzouzi, Olivier Cussenot

► **To cite this version:**

Pierre Bigot, Kevin Mouzat, Souhil Lebdai, Muriel Bahut, Nora Benhabiles, et al.. Quantitative proteomic determination of diethylstilbestrol action on prostate cancer. Asian Journal of Andrology, 2013, 15, pp.413-420. 10.1038/aja.2012.128 . hal-01543057

HAL Id: hal-01543057

<https://hal.sorbonne-universite.fr/hal-01543057>

Submitted on 20 Jun 2017

HAL is a multi-disciplinary open access archive for the deposit and dissemination of scientific research documents, whether they are published or not. The documents may come from teaching and research institutions in France or abroad, or from public or private research centers.

L'archive ouverte pluridisciplinaire **HAL**, est destinée au dépôt et à la diffusion de documents scientifiques de niveau recherche, publiés ou non, émanant des établissements d'enseignement et de recherche français ou étrangers, des laboratoires publics ou privés.



Distributed under a Creative Commons Attribution 4.0 International License

ORIGINAL ARTICLE

Quantitative proteomic determination of diethylstilbestrol action on prostate cancer

Pierre Bigot^{1,2}, Kevin Mouzat^{2,3}, Souhil Lebdaï¹, Muriel Bahut⁴, Nora Benhabiles⁵, Géraldine Cancel Tassin², Abdel-Rahmène Azzouzi¹ and Olivier Cussenot²

Diethylstilbestrol (DES) has a direct cellular mechanism inhibition on prostate cancer. Its action is independent from the oestrogen receptors and is preserved after a first-line hormonal therapy. We aimed to identify proteins involved in the direct cellular inhibition effects of DES on prostate cancer. We used a clonogenic assay to establish the median lethal concentration of DES on 22RV1 cells. 22RV1 cells were exposed to standard and DES-enriched medium. After extraction, protein expression levels were obtained by two-dimensional differential in-gel electrophoresis (2D-DIGE) and isotope labelling tags for relative and absolute quantification (iTRAQ). Proteins of interest were analysed by quantitative RT-PCR and western blotting. The differentially regulated proteins ($P < 0.01$) were interrogated against a global molecular network based on the ingenuity knowledge base. The 2D-DIGE analyses revealed DES-induced expression changes for 14 proteins (> 1.3 fold; $P < 0.05$). The iTRAQ analyses allowed the identification of 895 proteins. Among these proteins, 65 had a modified expression due to DES exposure (i.e., 23 overexpressed and 42 underexpressed). Most of these proteins were implicated in apoptosis and redox processes and had a predicted mitochondrial expression. Additionally, ingenuity pathway analysis placed the OAT and HSBP1 genes at the centre of a highly significant network. RT-PCR confirmed the overexpression of OAT ($P = 0.006$) and HSPB1 ($P = 0.046$).

Asian Journal of Andrology (2013) 15, 413–420; doi:10.1038/aja.2012.128; published online 25 February 2013

Keywords: cultured cells; DES; diethylstilbestrol; ingenuity pathway analysis; isotope labelling; mass spectrometry; prostate cancer; proteomics

INTRODUCTION

Existing evidence suggests that oestrogens may play a central role in prostate cancer (PCa) and that these oestrogens may initiate drivers of PCa progression. However, it seems paradoxical that oestrogens have been used to treat advanced PCa.¹ Diethylstilbestrol (DES) was the most commonly used hormonal therapy for PCa treatment between 1950 and 1980. Its side effects progressively led to halting its use for its primary intentions. DES is used currently as a second-line hormonal therapy. Several trials demonstrated a persistence of DES efficiency after a first-line hormonal therapy failure.^{2–8} It has been reported that prostate-specific antigen (PSA) levels decreased by more than half in 21%–86% of patients treated with DES. However, its side effects (e.g., thrombosis and cardiac toxicity) have hindered its use; even at a low dose (1 mg), toxicity was observed in almost 20% of patients.^{2–9} Several mechanisms for its action have been suggested, including the inhibition of the hypothalamo-pituitary axis by negative biofeedback, direct testosterone production inhibition by the testis and adrenal glands, and direct cytotoxicity on prostatic cancer cells. This direct effect mechanism is unknown, and identification of the responsible proteins may lead to the development of targeted therapies. This direct action has been reported in several studies that confirmed the *in vitro* cytotoxicity

of DES on PCa, LNCaP and PC-3 cells.^{10–12} Robertson *et al.*¹¹ also demonstrated that the oestradiol saturation of oestrogen receptors (ERs) prior to DES exposure did not affect its action, which confirmed the DES independence from the oestrogen receptors ER α and ER β . Similarly, even though androgen receptors play a central role in prostate carcinogenesis and disease progression, they do not appear to have any influence on DES action.¹³ Recently, 22RV1 cells became a major model for ligand-independent androgen receptor splice variants.^{14,15} This cell line has no oestrogen receptors (ER α and ER β), which permits studying the direct effects of DES.

Protein separation methods associated with mass spectrometry (MS) identification are new, powerful tools for the global analysis of the cellular and tissue proteomes. Thus, these techniques are useful for assessing gene expression and determining accurate protein expression rates, post-transcriptional modifications, interactions with other proteins and intracellular localisation.¹⁶ Methods associated with isobaric tagging, such as isobaric tagging reagent for absolute quantify (iTRAQ), a proteomic approach that allows the comparison of relative variations in cellular or tissular protein expression according to genetic modification, allow the analysis of protein changes in response to treatment or transformation.

¹Department of Urology, Angers University Hospital, Angers 49933, France; ²CeRePP, Tenon Hospital, Paris 75970, France; ³Department of Biochemistry, Nîmes University Hospital, Nîmes 30029, France; ⁴Plate-Forme Technologique de Biotechnologie Moléculaire, Angers University, Angers 49933, France and ⁵CEA, DSV, IRCM, SREIT, Laboratoire de Cancérologie Expérimentale, Fontenay-aux-Roses 92265, France
Correspondence: Dr P Bigot (pibigot@chu-angers.fr)

Received: 9 September 2012; Revised: 19 October 2012; Accepted: 29 October 2012; Published online: 25 February 2013

The aim of this study was to identify proteins implicated in the direct cytotoxic action of DES on 22RV1 prostate tumour cells using complementary quantitative proteomic approaches.

MATERIALS AND METHODS

Cell culture and reagent

The 22RV1 PCa cell line was grown in RPMI 1640 medium supplemented with 10% (v/v) foetal bovine serum without antibiotics in a 5% humidified CO₂ atmosphere at 37 °C. After a 24-h incubation, cells were treated for 48 h with 10 or 20 µmol l⁻¹ DES. Cells were retrieved by scraping, and cell pellets were then lysed in a solution containing 7 mol l⁻¹ urea, 2 mol l⁻¹ thiourea and 4% (w/v) CHAPS at 4 °C for 1 h under agitation. Lysis was achieved by sonication on ice (3×5 s pulses), and the lysates were clarified by centrifugation at 14 000 g at 4 °C for 15 min.

Clonogenicity evaluation of cell death induced by DES

Cells were grown in six-well plates as previously described and then treated with increasing DES concentrations ranging from 0 to 40 µmol l⁻¹. After 10 days, clones were washed with phosphate-buffered solution and then stained with 1 ml of crystal violet. Clones were then counted using Chemidoc XRS software. Six independent replicates were performed.

Two-dimensional differential in-gel electrophoresis (2D-DIGE)

(Figure 1)

22RV1 cells treated in the absence or presence of 10 or 20 µmol l⁻¹ DES were used for 2D-DIGE analysis. After extraction, proteins were purified using a 2D clean up kit (GE Healthcare, München, Germany) and resolubilized in 7 mol l⁻¹ urea, 2 mol l⁻¹ thiourea, 4% CHAPS and 30 m mol l⁻¹ Tris-HCl, pH 8.5 (DIGE lysis buffer). The proteins were then quantified using the Fluoroprofile kit. Internal standards were produced by pooling 25 µg of proteins from all samples. A total of 50 µg (10 µl) of protein samples were labelled at 4 °C for 30 min in the dark with 400 pmol Cy3 or Cy5 freshly reconstituted with dimethylformamide. Internal standard proteins (400 µg) were labelled with 3200 pmol Cy2. A quenching reaction was performed with 1 nmol l⁻¹ lysine for 10 min, and the proteins were diluted in one volume of 7 mol l⁻¹ urea, 2 mol l⁻¹ thiourea, 4% CHAPS, 2% dithiothreitol (DTT) and 2% immobilized pH gradient (IPG) buffer pH 3–11 NL

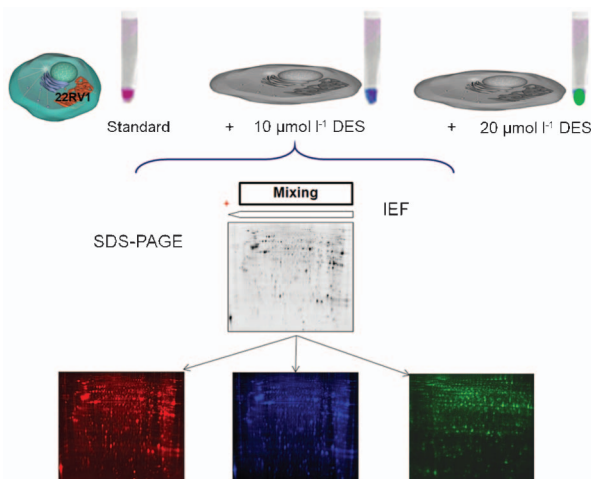


Figure 1 Workflow for the identification of 22RV1 cell proteomic changes after diethylstilbestrol treatment using DIGE labelling. DIGE, differential in-gel electrophoresis; IEF, isoelectric focusing; SDS-PAGE, sodium dodecyl sulphate-polyacrylamide.

(2× sample buffer). Pooling was performed according to the experimental design.

IEF (Ettan IPGphor 3; GE Healthcare) with 33 kVh was performed with sample cup-loading on 24 cm, pH 3–11 NL Immobiline DryStrips (GE Healthcare) initially rehydrated for 12 h with Destreak solution. Strip equilibration for 15 min in 50 mmol l⁻¹ Tris-HCl, pH 8.8, 6 mol l⁻¹ urea, 30% glycerol, 2% sodium dodecyl sulphate and 1% DTT was performed before replacement with 2.5% iodoacetamide for 15 min. Sodium dodecyl sulphate-polyacrylamide was performed using the Ettan DALTsix system (GE Healthcare) with home-made 12.5% acrylamide gels at 25 °C at 1 W/gel for 1 h then 17 W/gel.

A gel scan was performed with 100 µm resolution using an Ettan DIGE Imager (GE Healthcare), and images were analysed with Progenesis SameSpot software (non-linear dynamics) by picking spots with ≥1.3-fold change and *P*<0.05 directly from two pooled DIGE gels using Ettan Spot picker (GE Healthcare) and spot proteolysis was performed using the all-in-one trypsin digestion kit under a keratin-free atmosphere.

Afterward, desalted samples were analysed by MS and MS/MS using a 4800 MALDI-TOF/TOF Analyser (Applied Biosystems, Foster City, CA, USA). Spectra analysis was performed using the GPS Explorer software with the MASCOT search engine (Matrix Science) for protein identification with ≥95% confidence scores and ≥3 peptides using the human SwissProt database.

iTRAQ labelling (Figure 2)

Protein digestion and peptide labelling with iTRAQ reagents. 22RV1 cells treated in the absence and presence of 10 µmol l⁻¹ DES were used for iTRAQ analysis. Protein samples were purified by precipitation with six volumes of cold acetone at -20 °C overnight followed by the resuspension of pellets in 0.5 mol l⁻¹ triethylammonium bicarbonate, pH 8.5 and a final centrifugation step at 14 000 g at 4 °C for 15 min. We quantified the proteins from the supernatant with the 2D Quant Kit (GE Healthcare) before diluting the protein samples to 5 mg ml⁻¹ with triethylammonium bicarbonate buffer. We used 100 µg of proteins for further reduction, alkylation, digestion and iTRAQ labelling using iTRAQ Reagents Multiplex Kit (Applied Biosystems, Foster City, CA, USA) according to the manufacturer's protocol. Briefly, protein samples were reduced with 5 mmol l⁻¹ tris-(2-carboxyethyl) phosphine at 60 °C for 1 h, and the cysteine

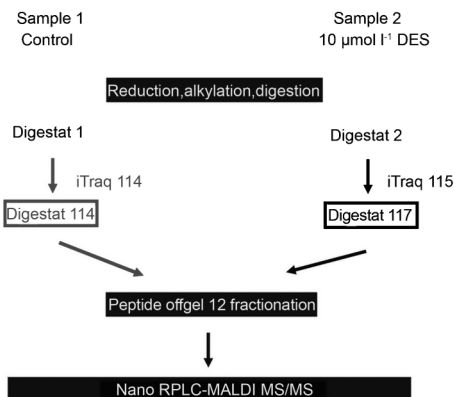


Figure 2 Workflow for the identification of 22RV1 proteomic after DES treatment using iTRAQ labelling. DES, diethylstilbestrol; iTRAQ, isotope labelling tags for relative and absolute quantification.

groups were blocked using a 10 mmol l⁻¹ methyl methanethiosulfonate solution at room temperature for 10 min. The proteins were then digested with 10 µg of trypsin at 37 °C for 16 h. Each peptide solution was labelled at room temperature for 1 h with one iTRAQ reagent vial (mass tag 114 or 115) that was previously reconstituted with 70 µl of ethanol. Samples of the same protein content were labelled with 114 and 115 iTRAQ reagents and combined, and the labelling reaction was halted by evaporation in a Speed Vac to obtain a brown pellet.

Peptide OFFGEL fractionation. For pI-based peptide separation, we used a 3100 OFFGEL Fractionator (Agilent Technologies, Böblingen, Germany) with a 12-well set-up. Prior to electro focusing, samples were desalted onto a Sep-Pak C18 cartridge (Waters). For the 12-well set-up, peptide samples were diluted to a final volume of 3.6 ml using the OFFGEL peptide sample solution. To begin, the IPG gel strips (24 cm-long with a 3–10 linear pH range) (GE Healthcare) were rehydrated with the Peptide IPG Strip Rehydration Solution according to the protocol of the manufacturer for 15 min. Then, 150 µl of sample was loaded into each well. Electro focusing of the peptides was performed at 20 °C and 50 µA until the 50 kWh level was reached. After focusing, the 24-peptide fractions were withdrawn, the wells were rinsed with 200 µl of water/methanol/formic acid (49/50/1) after 15 min and the rinsing solutions were pooled with their corresponding peptide fraction. All fractions were evaporated by centrifugation under vacuum and maintained at -20 °C. Just prior to the nano-LC, the fractions were resuspended in 20 µl of H₂O with 0.1% (v/v) TFA.

Capillary LC separation. The samples were separated on an Ultimate 3000 nano-LC system (Dionex) using a C18 column (PepMap100; 3 µm, 100 Å, 75 µm id×15 cm; Dionex, Sunnyvale, CA, USA) at a 300 nl min⁻¹ flow rate. Buffer A included 2% ACN in water with 0.05% TFA and buffer B was 80% ACN in water with 0.04% TFA. The peptides were desalted for 3 min using only buffer A on the precolumn followed by separation for 60 min using the following gradient: 0%–20% B for 10 min, 20%–55% B for 45 min and 55%–100% B for 5 min. Chromatograms were recorded at 214 nm, and peptide fractions were collected using a Probot microfraction collector (Dionex). For SCX fractionation, we used salt gradient steps: 20-µl injections of 5, 10, 25, 50, 75, 100, 125, 150, 200, 300, 500 and 1000 mmol l⁻¹ NaCl. We used CHCA (LaserBioLabs, Sophia-Antipolis, France) as a MALDI matrix. The matrix (2 mg ml⁻¹ in 70% ACN in water with 0.1% TFA) was continuously added to the column effluent via a micro 'T' mixing piece at a 1.2 µl min⁻¹ flow rate. After a 14-min run, a start signal was sent to the Probot to initiate fractionation. Fractions were collected for 10 s and spotted onto an MALDI sample plate (1664 spots per plate; Applied Biosystems, Foster City, CA, USA).

MALDI-MS/MS

MS and MS/MS analyses of off-line-spotted peptide samples were performed using a 4800 MALDI-TOF/TOF Analyser (Applied Biosystems, Foster City, CA, USA). After screening all of the LC-MALDI sample positions in MS-positive reflector mode using 1500 laser shots, the fragmentation of automatically selected precursors was performed at 1 kV collision energy using air as the collision gas (~2×10⁻⁶ Torr). MS spectra were acquired between 800 and 4000 m/z. For internal calibration, we used the Glu1-fibrinopeptide parent ion at 1570.677 m/z diluted in the matrix (3 femtomoles per spot). Up to 12 of the most intense ion signals per spot position

having an S/N >12 was selected as precursors for MS/MS acquisition. Peptide and protein identification were performed by the ProteinPilot™ Software V 2.0 (Applied Biosystems, Foster City, CA, USA) using the Paragon algorithm. Each MS/MS spectrum was searched against the Uniprot/swissprot database (release 51, October 2006) for *Homo sapiens*. The searches were run with the fixed modification of methylmethanethiosulfate-labelled cysteine parameter enabled. Other parameters such as tryptic cleavage specificity, precursor ion mass accuracy and fragment ion mass accuracy are MALDI 4800 built-in functions of the ProteinPilot software.

The ProteinPilot software calculates a confidence percentage (the unused score), which reflects the probability that a hit is a false positive, meaning that at a 95% confidence level, there is a false positive identification chance of approximately 5%. While this software automatically accepts all peptides having an identification confidence level >1%, only proteins having at least one peptide above the 95% confidence level were initially recorded. Low confidence peptides cannot provide positive protein identification by themselves, but may support the presence of a protein identified using other peptides with higher confidence. Performing a search with a concatenated database containing forward and reversed sequences allowed an estimation of the false discovery rate below 1%. The experimental pI for each peptide was calculated using the pI/Mw tool on the Expasy Proteomic Server.¹⁷

Real-time PCR

Total RNA was isolated using the RNeasy Mini Kit (Qiagen, Courtaboeuf, France) according to the manufacturer's instructions. cDNA was synthesized from 1 µg of total RNA with SuperScript III (Invitrogen, Cergy-Pontoise, France) and random hexamer primers according to the manufacturer's recommendations. Real-time PCR was performed on a 7500 Real-Time PCR System (Applied Biosystems, Courtaboeuf, France) using Power SYBR Green PCR Master Mix according to manufacturer's instructions. Gene expression measurements were calculated using a calibration curve on each run. The calibration curve consisted of cDNA serial dilutions obtained from QPCR Human Reference total RNA (Ozyme, Saint-Quentin-en-Yvelines, France). Each point was run in triplicate and normalised to the expression of the HPRT gene. Primer sequences for ESR2, Ornithine Aminotransferase (OAT) and IGFBP2 were provided by RTPprimerDB.¹⁸ For qRT-PCR analysis, the *t*-test was performed to determine whether there were differences between the groups. A *P*<0.05 was considered significant.

Western blotting

Cells were manually scrapped and lysed in a buffer composed of 7 mol l⁻¹ urea, 2 mol l⁻¹ thiourea and 4% CHAPS for 1 h at 4 °C. Lysis was completed by sonication (3 cycles of 5 s). Quantification was performed by fluorometry by using the fluoroprofile kit (Sigma-Aldrich, Saint Louis, MO, USA). Protein samples (100 µg) were separated on a 12% polyacrylamide-sodium dodecyl sulphate gel. The proteins were then transferred onto a PVDF membrane. The membrane was saturated with a solution containing 3% BSA in TBS (0.1 mol l⁻¹, pH=7.4). Blots were then incubated with the proper antibodies (1/200 dilution) at 4 °C overnight. β-tubulin was used as a charge control and was incubated with a specific rabbit polyclonal antibody (sc-9104; Santa Cruz Biotechnology Inc., Santa Cruz, CA, USA). The membranes were then incubated with a secondary antibody conjugated with a peroxidase (goat anti-rabbit IgG, 1:5000; Santa Cruz Biotechnology Inc.).

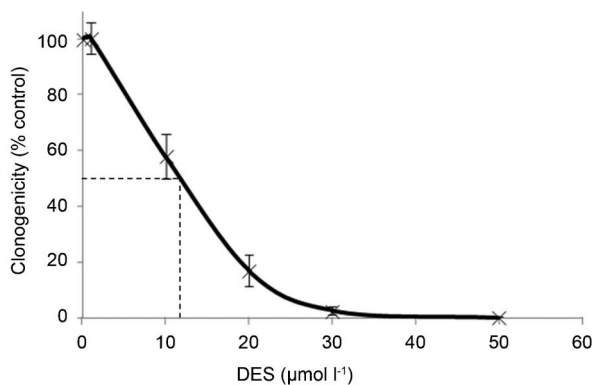


Figure 3 Cell survival curve. The median lethal DES concentration for 22RV1 cells was 11.75 $\mu\text{mol l}^{-1}$. DES, diethylstilbestrol.

Polyclonal anti-OAT (sc-55732; Santa Cruz Biotechnology Inc.) was used for western blotting, and the experiment was repeated three times to confirm the results.

Ingenuity pathway analysis (IPA)

The differentially regulated proteins ($P < 0.01$) were overlaid onto a global molecular network developed from information contained in the ingenuity knowledge base (Ingenuity Systems®, <http://www.ingenuity.com>, content version 12402621, release date: 2012-03-09). Networks of these proteins were then algorithmically generated based on their connectivity. Biological functions associated with proteins within the newly formed networks were displayed using the functional analysis feature in the order of their significance to the network. If the significance of the association between the network and the biological function had a $P < 0.05$, then the biological function was displayed in the functional analysis feature. The IPA was based on the ingenuity knowledge base (i.e., genes plus endogenous chemicals), and direct and indirect relationships were included with a filter set-up so that confidence equalled to that experimentally observed.

RESULTS

Clonogenic assay

Clonogenic assay revealed that the median lethal concentration of DES for 22RV1 cells was 11.75 $\mu\text{mol l}^{-1}$ (Figure 3).

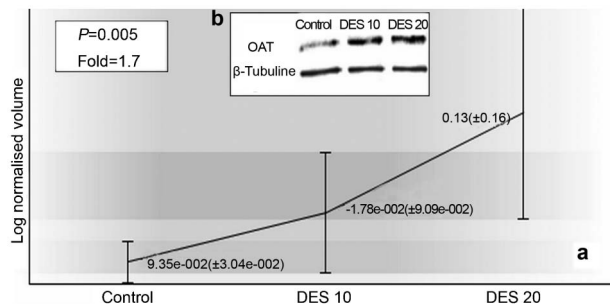


Figure 4 OAT was overexpressed in 22RV1 DES-treated cells in 2D-DIGE (a) and western blotting (b). DES, diethylstilbestrol; OAT, ornithine aminotransferase; 2D-DIGE, two-dimensional differential in-gel electrophoresis.

Cell culture

After identifying the median lethal DES concentration by clonogenic assay, we chose to study the DES effects on 22RV1 cells at 10 $\mu\text{mol l}^{-1}$ (2D-DIGE and iTRAQ) and 20 $\mu\text{mol l}^{-1}$ (2D-DIGE) treatments for 24 h to obtain a specific response.

2D-DIGE

Among the 1087 proteins spots identified in the electrophoresis gel, replicate analysis of fluorescent images from six independent gels revealed a change in the expression of 14 proteins induced by DES ($P < 0.05$; > 1.3 -fold) (Table 1). Fourteen spots were identified by MALDI-TOF/TOF MS. Eight proteins were overexpressed and seven proteins were underexpressed. The identified proteins are involved in diverse processes including intracellular signalling, oxidation/reduction, apoptosis, DNA replication and microtubule DE polymerisation. Of these proteins, we confirmed the overexpression of OAT by western blotting (Figure 4).

iTRAQ

After three replicate proteomic analyses, 895 constitutive proteins in the 22RV1 proteome were identified. Among these proteins, 65 were differentially expressed in response to DES exposure (23 overexpressed and 42 underexpressed) (Table 2). Most of these proteins have been implicated in apoptosis and redox processes and have a predicted mitochondrial expression.

Table 1 Proteins significantly altered in response to DES upon 2D-DIGE analysis

	P	Fold	Variation ^a	Gene symbol	Identification
1	0.023	1.8	-	DUT	Deoxyuridine 5'-triphosphate nucleotidohydrolase
2	0.05	1.8	-	STMN1	Stathmin
3	0.028	1.7	-	DPYSL2	Dihydropyrimidinase-related protein
4	0.014	1.5	-	COPE	Coatomer subunit epsilon
5	0.022	1.4	-	TMPO	Lamina-associated polypeptide 2 isoform alpha
6	0.024	1.3	-	PAK2	Serine/threonine-protein kinase 2
7	0.005	1.7	+	OAT	OAT
8	0.038	1.5	+	CTNND1	Catenin delta-1
9	0.027	1.4	+	SND1	Staphylococcal nuclease domain-containing protein
10	0.006	1.4	+	CCDC130	Poly(rC)-binding protein
11	0.012	1.3	+	CHDH	Choline dehydrogenase, mitochondrial
12	0.042	1.3	+	TOMM70A	Mitochondrial import receptor subunit TOM70
13	0.039	1.3	+	UGDH	UDP-glucose 6-dehydrogenase
14	0.031	1.6	+	N.I	N.I

Abbreviations: DES, diethylstilbestrol; OAT, ornithine aminotransferase; 2D-DIGE, two-dimensional differential in-gel electrophoresis.

^a +: upregulated; -: downregulated.

Table 2 Proteins significantly altered in response to DES upon i-TRAQ analysis

No.	Protein name	Gene symbol	DES 10 $\mu\text{mol l}^{-1}$ /control fold change	Regulation ^a
1	Eukaryotic translation initiation factor 4E-binding protein 2	EIF4EBP2	2.29	+
2	Eukaryotic translation initiation factor 5A-1	EIF5A	2.29	+
3	Heat shock protein beta-1	HSPB1	2.17	+
4	Histone H2B type 1-L	HIST1H2BL	2.01	+
5	Hsc70-interacting	ST13	1.97	+
6	Eukaryotic translation initiation factor 1A	EIF1AX	1.83	+
7	Heat shock protein beta-6	HSPB6	1.82	+
8	Fatty acid-binding protein, epidermal	FABP5	1.81	+
9	Histone H3.1t	HIST3H3	1.79	+
10	Thymosin beta-10	TMSB10	1.76	+
11	Microfibrillar-associated protein 1	MFAP1	1.73	+
12	Cofilin-1	CFL1	1.68	+
13	Nucleoside diphosphate kinase A	NME1	1.66	+
14	14-3-3 protein zeta/delta	YWHAZ	1.63	+
15	Enoyl-CoA hydratase, mitochondrial	ECHS1	1.61	+
16	DnaJ homolog subfamily C member 8	DNAJC8	1.59	+
17	Creatine kinase B-type	CKB	1.55	+
18	Creatine kinase, ubiquitous mitochondrial	CKMT1A	1.54	+
19	Keratin, type II cytoskeletal 8	KRT8	1.50	+
20	Heterogeneous nuclear ribonucleoprotein G	HNRNPM	1.44	+
21	Peptidyl-prolyl cis-trans isomerase A	PPIA	1.39	+
22	Glucosidase 2 subunit beta	PRKCSH	1.34	+
23	Nucleolin	NCL	1.29	+
24	Calmodulin	CALM1	0.666	-
25	Non-histone chromosomal protein HMG-17	HMGN2	0.655	-
26	Keratin, type I cytoskeletal 10	KRT10	0.65	-
27	Serine protease hepsin	HPN	0.62	-
28	Transcription elongation factor A protein 1	TCEA1	0.618	-
29	Polypeptide N-acetylgalactosaminyltransferase 2	GALNT2	0.613	-
30	Acyl carrier protein, mitochondrial	NDUFAB1	0.599	-
31	Ras-related protein Rab-5C	RAB5C	0.596	-
32	Lamin-B1	LMNB1	0.595	-
33	Cleavage stimulation factor 64 kDa	CSTF2	0.587	-
34	26S proteasome non-ATPase regulatory subunit 9	PSMD9	0.584	-
35	60S acidic ribosomal protein P2	RPLP2	0.581	-
37	Coiled-coil domain-containing protein 12	CCDC12	0.573	-
38	Heme-binding protein 1	HEBP1	0.564	-
39	Cytochrome c1	CYC1	0.557	-
40	Cob(II)yrinic acid, mitochondrial	MMAB	0.555	-
41	Transcriptional repressor CTCF	CTCF	0.552	-
42	Thioredoxin reductase 2, mitochondrial	TXNRD2	0.534	-
43	Gamma-glutamyl hydrolase	GGH	0.509	-
44	Putative histone H2B type 2-D	HIST2H2BD	0.506	-
45	Complement component 1 Q	C1QBP	0.504	-
46	Fox-1 homolog A	RBFOX1	0.493	-
47	60S ribosomal protein L37	RPL37	0.491	-
48	Cysteine and glycine-rich protein 2	CSRP2	0.491	-
49	Developmentally-regulated GTP-binding protein 1	DRG1	0.483	-
50	Death-inducer obliterator 1	DIDO1	0.482	-
51	Keratin, type II cytoskeletal 1	KRT1	0.48	-
52	Beta-lactamase-like protein 2	LACTB2	0.466	-
53	Glutathione synthetase	GSS	0.453	-
54	Cyclin-dependent kinases regulatory subunit 1	CKS1B	0.449	-
55	Glutathione reductase, mitochondrial	GSR	0.44	-
56	UPF0424 protein C1orf128	PP7435	0.435	-
57	Insulin-like growth factor-binding protein 2	IGFBP2	0.416	-
58	High mobility group protein HMG-I/HMG-Y	HMGA1	0.412	-
59	Keratin, type I cytoskeletal 9	KRT9	0.406	-
60	Very long-chain specific acyl-CoA dehydrogenase	ACADVL	0.37	-
61	Histone H2B type 1-H	HIST1H2BH	0.281	-
62	Lamina-associated polypeptide 2, isoform alpha	TMPO	0.307	-
63	Eukaryotic translation initiation factor 5A-1-like	EIF5AL1	0.342	-
64	Actin	ACTA1	0.3	-
65	Dihydrolipoyl dehydrogenase, mitochondrial	DLD	0.257	-

Abbreviations: DES, diethylstilbestrol; iTRAQ, isotope labelling tags for relative and absolute quantification.

^a +: upregulated; -: downregulated.

RT-PCR

Gene expression analysis confirmed that the oestrogen receptors ESR1 and ESR2 were not expressed in our model (data not shown). We assessed the expression of OAT, heat shock protein beta-1 (HSPB1) and insulin-like growth factor-binding protein 2 (IGFBP2) by RT-PCR. These proteins were identified by 2D-DIGE and iTRAQ and are known to be implicated in natural progression of PCa. The expression of these proteins was changed by DES exposure according to the proteomic analysis. The analysis confirmed the overexpression of OAT ($P=0.006$) and HSPB1 ($P=0.046$). However, the variation of IGFBP2 was inconsistent; it was underexpressed according to the iTRAQ analysis and overexpressed by RT-PCR ($P=0.011$). These findings suggest that DES exerts both transcriptional and post-transcriptional effects on 22RV1 cells (Figure 5).

IPA

The network analysis output from IPA provides an additional indication of the link between proteins (expression changes by DES) and cellular processes such as apoptosis. IPA revealed that many of the up/downregulated genes in the profile bind together, regulate each other, and play a common role in oxidative stress.

The top deregulated network functions were associated with genetic disorder, cell death, cellular movement, carbohydrate and nucleic acid metabolism, cellular growth and proliferation and cellular assembly and organisation. A consensus network of the 65 proteins significantly deregulated was constructed with ingenuity as shown in Figure 6 (green biomarkers are downregulated while red biomarkers are up-regulated). This figure demonstrates the direct and indirect known relationships between the biomarkers deregulated in the experiment.

DISCUSSION

Oestrogen effects have been widely studied in metastatic PCa, particularly as a second-line treatment following resistance to luteinizing hormone-releasing hormone analogues.¹⁹ Several mechanisms have been suggested, including inhibition of the hypothalamo-pituitary axis by negative biofeedback, direct testosterone production inhibition by the testis and adrenal glands, and direct cytotoxicity on prostatic cancer cells. These mechanisms were reported in several studies that exposed the *in vitro* cytotoxicity of DES on the PCa cell lines LNCaP and PC-3.^{10–12,20} Oestrogen effects are mainly mediated by nuclear ER. Two ER subtypes have been isolated in the prostate: ER α , which is mainly expressed in the stromal compartment, and ER β expressed in the epithelium. These isoforms are produced by two different genes: ER α (which is encoded by chromosome 6q25.181) and ER β (which is encoded by chromosome 14q22–24).^{21,22} Robertson *et al.*¹¹ confirmed the independence of the DES

effects on these oestrogen receptors (ER α and ER β) by saturating them with estradiol prior to DES exposure. Our study confirms this direct DES cytotoxicity on 22RV1 cells. According to clonogenicity tests, the median lethal dose of DES on 22RV1 cells was $11.75 \mu\text{mol l}^{-1}$. This action was independent of oestrogen receptors as 22RV1 cells did not express these proteins. These results confirm the previous findings.

To identify the proteins involved in the DES mechanism, we used a proteomic approach combining 2D-DIGE and iTRAQ. These two methods are complementary. The proteins are separated and quantified prior to digestion and identification with 2D-DIGE, which is different from the iTRAQ method, which employs digestion prior to quantification. Wu *et al.*²³ demonstrated the complementary aspect of these two techniques in a global analysis of the cellular and tissue proteome. We highlighted this complementary approach by 2D-DIGE identification and iTRAQ analysis for the proteins differentially expressed in response to DES.

Of the 14 proteins identified by 2D-DIGE, we validated the DES-mediated OAT overexpression by western blotting and RT-PCR. OAT is a mitochondrial enzyme involved in the metabolism of arginine that catalyses the conversion of L-ornithine and 2-oxo acid to L-glutamate 5-semialdehyde and an L-amino acid. OAT is an essential enzyme for the metabolism of polyamines, which are molecules implicated in the proliferation and survival of PCa cells.^{24,25} OAT expression is increased in hormone-resistant PCa cells and appears to compensate for the arginase II decrease during polyamine production.²⁶ The OAT gene is also regulated by the androgen receptor, and it has been shown that OAT expression decreased on rat kidneys after testosterone exposure.²⁷ The implication of OAT in the natural progression of PCa appears to be relevant and requires examination by complementary studies to identify its function in the DES treatment response.

After three iTRAQ analyses, we were able to reliably identify 895 proteins. These proteins were the most abundant in the 22RV1 cell proteome. Among these proteins, 65 had significantly modified expression due to DES exposure (i.e., 23 overexpressed and 42 underexpressed). These proteins are mainly implicated in redox regulation, the synthesis and transcription of DNA, apoptosis, the constitution and modification of the cytoskeleton, and ionic transport. The increase in cytochrome c and several pro-apoptotic factors may suggest that apoptosis could be induced by the caspase pathway and activated by oxidative stress. Network analysis using IPA provides another indication for the link between these proteins and cellular processes such as apoptosis. IPA confirms that many of the up/downregulated proteins bind and regulate each other and also play a common role in oxidative stress.

Among the identified proteins, we focussed on those that had a modified expression induced by DES, particularly those involved in natural PCa progression.

Heat shock protein 27 (HSPB1) is a 27 kDa stress protein involved in cytoskeleton stability. This protein also has antiapoptotic activity that involves inhibiting cytochrome c and the formation of the apoptosome, which is responsible for caspase activation. HSPB1 also contributes to cell survival by activating the AKT protein and inhibiting the apoptosis induced by BAX and also by reinforcement of the NF-KB pathway.^{28–30} HSPB1 was originally discovered as an oestrogen-modulated breast cancer protein³¹ and was recently identified as a pejorative PCa prognostic marker.³² The HSPB1 level increases after androgen suppression and is cytoprotective in hormone-refractory PCa.^{33,34} In our study, the HSPB1 increase was

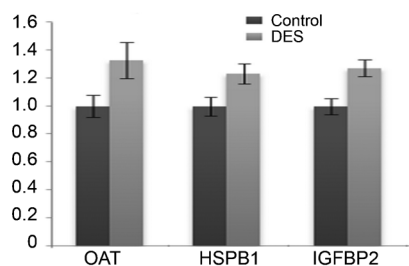


Figure 5 Variations of the identified proteins of interest by quantitative RT-PCR. Transcripts were quantified by qRT-PCR analysis (mean \pm s.e.). $n=5$ in each group. DES, diethylstilbestrol; OAT, ornithine aminotransferase.

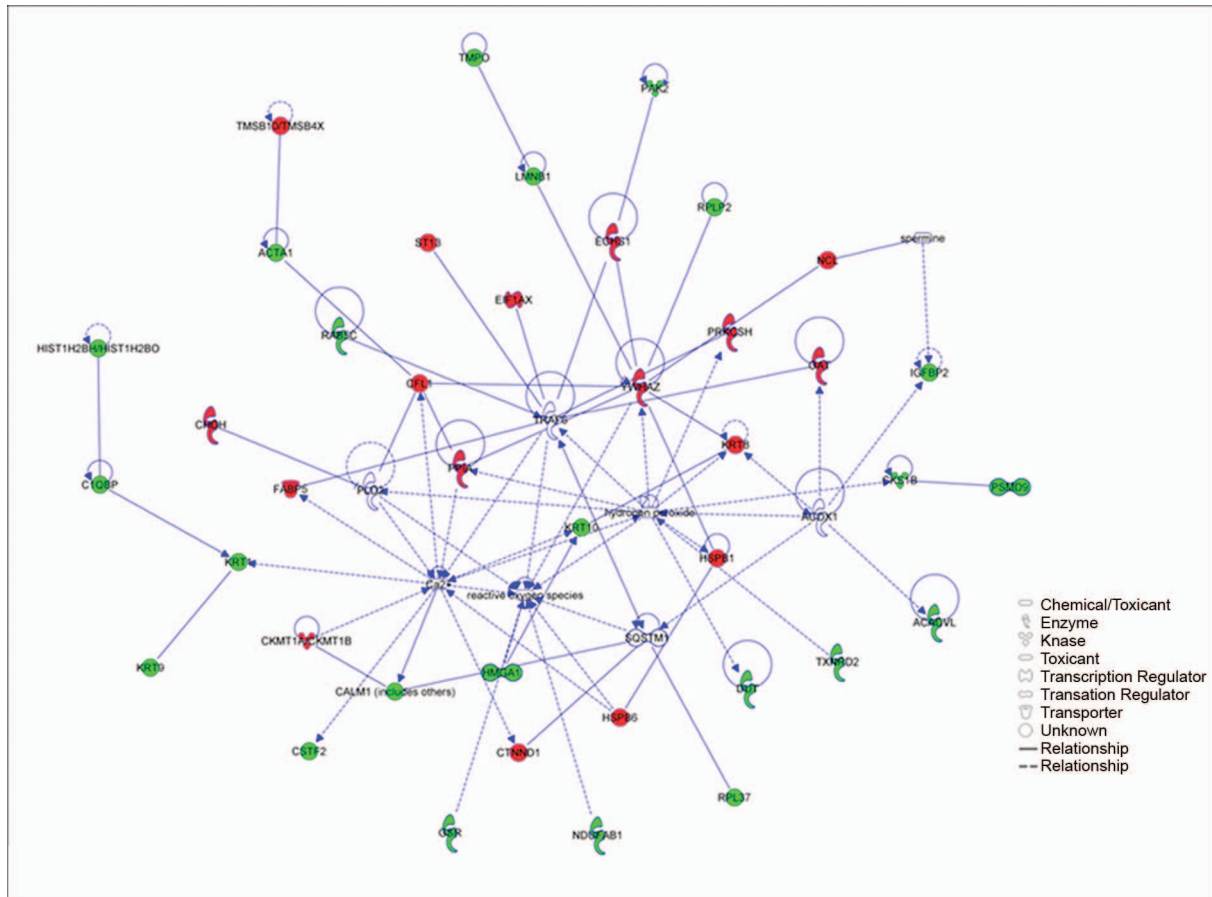


Figure 6 Network analysis output of the IPA core analysis. The green colour reflects gene expression downregulation, and red represents upregulation. The network analysis output from IPA provides yet another indication of the association between the proteins (expression changes by DES) and cellular processes such as apoptosis. IPA reveals that many of the up/downregulated genes in the profile bind and regulate each other and play a common role in oxidative stress. DES, diethylstilbestrol; IPA, ingenuity pathway analysis.

shown by iTRAQ analysis and qRT-PCR, suggesting its implication in the natural progression of PCa and the tumour response to DES.

The members of the growth hormone-insulin-like growth factor (IGF) axis possess numerous actions in cell proliferation, growth, survival, angiogenesis, chemoresistance and cross-talk signalling involving steroid hormone receptors and other growth factor receptor signalling cascades. The IGF axis consists of two ligands, two receptors and a family of closely related IGF binding proteins (IGFBP1–6).³⁵ The altered expression of IGF axis members is generally considered to be associated with the development of several cancers including PCa.^{36,37} Several reports have demonstrated an important role for IGFBP-2 in androgen insensitivity and the proliferation of PCa cells *in vivo*.³⁸ Recently Uzoh *et al.*³⁹ found that IGFBP2 plays a key role in the growth of PCa cells. Upon the silencing of IGFBP-2 expression, the resistance of these cells to docetaxel was reduced. In our study, we demonstrated a decrease in IGFBP-2 expression in response to DES by iTRAQ analysis. However, RT-PCR results demonstrated an increase in the IGFBP2 mRNA level. This finding may suggest that DES induces transcriptional and post-transcriptional effects in 22RV1 cells, which remains to be explored.

This study was the first to investigate the action of DES on a prostate cell line by a proteomic approach, and it also highlights the possibility of an induced oxidative pathway. Koike *et al.*¹² assessed the gene expression profiles of the PCa cells PC-3 and LNCaP after DES treatment. These

authors demonstrated that the expression of many genes including cell attachment, cell cycle, intracellular signalling, apoptosis and cell proliferation genes was downregulated after DES treatment. However, this group did not find that the same genes were implicated in the DES action. In another study, Geier *et al.*⁴⁰ demonstrated the ability of DES to inhibit telomerase in the PCa cell lines PC-3 and LNCaP. Cavalieri *et al.*⁴¹ suggested the possibility of several types of indirect DNA damage caused by oestrogen-induced oxidants. DES induced numerical and structural chromosome aberrations and several types of gene mutations in cells *in vitro* and *in vivo*. The formation of reactive oxygen species by oestrogens and the resulting indirect DNA damage by these oxidants may not only explain the hypothesis of induced PCa by clastogenicity due to oestrogens but also the paradoxical ability of these oestrogens to induce the apoptosis of PCa cells at high concentrations.

Unfortunately, our study is limited by the fact that we used only one cell line due to the difficulty and cost of proteomic analysis. However, the proteomic approach allows us to propose new proteins implicated in the DES mechanism of action. The specificity of these proteins in DES action requires validation in other studies.

We identified 78 proteins implicated in the response of 22RV1 cell lines to DES. These proteins require confirmation by other studies to validate their specificity in DES action. However, similar to the report of Robertson *et al.*¹¹ in 1996, we observed that DES cytotoxicity was

linked with a modification in the cellular architecture and the induction of apoptosis. The presence of a large number of mitochondrial proteins in redox reactions suggests the involvement of oxidative stress in DES response mechanisms. IPA confirmed a strong link between up/downregulated proteins, apoptosis and oxidative stress and has placed OAT and HSBP1 at the centre of a highly significant network.

CONCLUSION

The complementary proteomic approaches 2D-DIGE and iTRAQ analysis allowed us to identify 78 proteins whose expression depended on the presence of DES. Among these proteins, several mitochondrial proteins were identified. This finding suggests that DES may induce apoptosis by oxidative stress. The overexpression of OAT and HSBP1 has been confirmed by genomic and proteomic analysis. Additionally, IPA has placed OAT and HSBP1 at the centre of a highly significant network.

AUTHOR CONTRIBUTIONS

PB performed the proteomic study, the proteomic analysis and drafted the manuscript. KM performed the genetic studies and assisted in drafting the manuscript. SL assisted in drafting the manuscript. MB participated in 2D-DIGE analysis. NB performed the IPA. GCT participated in the design and coordination of the genetics studies. ARA participated in the design and coordination of the study. OC conceived and coordinated the study. All authors read and approved the final manuscript.

COMPETING FINANCIAL INTERESTS

All authors declare that there are no competing financial interests.

ACKNOWLEDGMENTS

This study was funded by the Association Française d'Urologie (AFU) and the Association pour la recherche sur les tumeurs de la prostate (ARTP).

- Singh PB, Matanhelia SS, Martin FL. A potential paradox in prostate adenocarcinoma progression: oestrogen as the initiating driver. *Eur J Cancer* 2008; **44**: 928–36.
- Scherr DS, Pitts WR Jr. The nonsteroidal effects of diethylstilbestrol: the rationale for androgen deprivation therapy without estrogen deprivation in the treatment of prostate cancer. *J Urol* 2003; **170**: 1703–8.
- Farrugia D, Ansell W, Singh M, Philp T, Chingwundoh F *et al*. Stilboestrol plus adrenal suppression as salvage treatment for patients failing treatment with luteinizing hormone-releasing hormone analogues and orchiectomy. *BJU Int* 2000; **85**: 1069–73.
- Smith DC, Redman BG, Flaherty LE, Li L, Strawderman M *et al*. A phase II trial of oral diethylstilbestrol as a second-line hormonal agent in advanced prostate cancer. *Urology* 1998; **52**: 257–60.
- Hellerstedt B, Pienta KJ, Redman BG, Esper P, Dunn R *et al*. Phase II trial of oral cyclophosphamide, prednisone, and diethylstilbestrol for androgen-independent prostate carcinoma. *Cancer* 2003; **98**: 1603–10.
- Montgomery RB, Nelson PS, Lin D, Ryan CW, Garzotto M *et al*. Diethylstilbestrol and docetaxel: a Phase II study of tubulin active agents in patients with metastatic, androgen-independent prostate cancer. *Cancer* 2007; **110**: 996–1002.
- Byar DP. Proceedings: The Veterans Administration Cooperative Urological Research Group's studies of cancer of the prostate. *Cancer* 1973; **32**: 1126–30.
- Oh WK. The evolving role of estrogen therapy in prostate cancer. *Clin Prostate Cancer* 2002; **1**: 81–9.
- Bosset PO, Albiges L, Seisen T, de la Motte Rouge T, Phe V *et al*. Current role of diethylstilbestrol in the management of advanced prostate cancer. *BJU Int*, e-pub ahead of print 11 May 2012; doi:10.1111/j.1464-410X.2012.11206.x.
- Malkowicz SB. The role of diethylstilbestrol in the treatment of prostate cancer. *Urology* 2001; **58**: 108–13.
- Robertson CN, Roberson KM, Padilla GM, O'Brien ET, Cook JM *et al*. Induction of apoptosis by diethylstilbestrol in hormone-insensitive prostate cancer cells. *J Natl Cancer Inst* 1996; **88**: 908–17.
- Koike H, Ito K, Takezawa Y, Oyama T, Yamanaka H *et al*. Insulin-like growth factor binding protein-6 inhibits prostate cancer cell proliferation: implication for anticancer effect of diethylstilbestrol in hormone refractory prostate cancer. *Br J Cancer* 2005; **92**: 1538–44.
- Koochekpour S. Androgen receptor signaling and mutations in prostate cancer. *Asian J Androl* 2010; **12**: 639–57.
- Visakorpi T, Hyytinen E, Koivisto P, Tanner M, Keinänen R *et al*. In vivo amplification of the androgen receptor gene and progression of human prostate cancer. *Nat Genet* 1995; **9**: 401–6.
- Sramkoski RM, Pretlow TG 2nd, Giaconia JM, Pretlow TP, Schwartz S *et al*. A new human prostate carcinoma cell line, 22Rv1. *In Vitro Cell Dev Biol Anim* 1999; **35**: 403–9.
- Comuzzi B, Sadar MD. Proteomic analyses to identify novel therapeutic targets for the treatment of advanced prostate cancer. *Cellscience* 2006; **3**: 61–81.
- Gasteiger E, Gattiker A, Hoogland C, Ivanyi I, Appel RD *et al*. ExPASy: the proteomics server for in-depth protein knowledge and analysis. *Nucleic Acids Res* 2003; **31**: 3784–8.
- Lefever S, Vandesompele J, Speleman F, Pattyn F. RTPrimerDB: the portal for real-time PCR primers and probes. *Nucleic Acids Res* 2009; **37**: D942–5.
- Huggins CB, Hodges CV. Studies on prostate cancer: the effects of castration, of estrogen and androgen injection on serum phosphatases in metastatic carcinoma of the prostate. *Cancer Res* 1941; **1**: 293–7.
- Li Y, Hwang TH, Oseth LA, Hauge A, Vessella RL *et al*. AR intragenic deletions linked to androgen receptor splice variant expression and activity in models of prostate cancer progression. *Oncogene* 2012; **31**: 4759–67.
- Leav I, Lau KM, Adams JY, McNeal JE, Taplin ME *et al*. Comparative studies of the estrogen receptors beta and alpha and the androgen receptor in normal human prostate glands, dysplasia, and in primary and metastatic carcinoma. *Am J Pathol* 2001; **159**: 79–92.
- Menasce LP, White GR, Harrison CJ, Boyle JM. Localization of the estrogen receptor locus (ESR) to chromosome 6q25.1 by FISH and a simple post-FISH banding technique. *Genomics* 1993; **17**: 263–5.
- Wu WW, Wang G, Baek SJ, Shen RF. Comparative study of three proteomic quantitative methods, DIGE, cIAT, and iTRAQ, using 2D gel- or LC-MALDI TOF/TOF. *J Proteome Res* 2006; **5**: 651–8.
- Cipolla BG, Ziade J, Bansard JY, Staerman F *et al*. Pretherapeutic erythrocyte polyamine spermine levels discriminate high risk relapsing patients with M1 prostate carcinoma. *Cancer* 1996; **78**: 1055–65.
- Pegg AE, McCann PP. Polyamine metabolism and function. *Am J Physiol* 1982; **243**: C212–21.
- Mumenthaler SM, Yu H, Tze S, Cederbaum SD, Pegg AE *et al*. Expression of arginase II in prostate cancer. *Int J Oncol* 2008; **32**: 357–65.
- Mueckler MM, Moran S, Pitot HC. Transcriptional control of ornithine aminotransferase synthesis in rat kidney by estrogen and thyroid hormone. *J Biol Chem* 1984; **259**: 2302–5.
- Konishi H, Matsuzaki H, Tanaka M, Takemura Y, Kuroda S *et al*. Activation of protein kinase B (Akt/RAC-protein kinase) by cellular stress and its association with heat shock protein Hsp27. *FEBS Lett* 1997; **410**: 493–8.
- Garrido C, Bruey JM, Fromentin A, Hammann A, Arrigo AP *et al*. HSP27 inhibits cytochrome c-dependent activation of procaspase-9. *FASEB J* 1999; **13**: 2061–70.
- Bruey JM, Ducasse C, Bonniaud P, Ravagnan L, Susin SA *et al*. Hsp27 negatively regulates cell death by interacting with cytochrome c. *Nat Cell Biol* 2000; **2**: 645–52.
- Adams DJ, Edwards DP, McGuire WL. Estrogen regulation of specific proteins as a mode of hormone action in human breast cancer. *Biomembranes* 1983; **11**: 389–414.
- Foster CS, Dodson AR, Ambroisine L, Fisher G, Moller H *et al*. Hsp-27 expression at diagnosis predicts poor clinical outcome in prostate cancer independent of ETS-gene rearrangement. *Br J Cancer* 2009; **101**: 1137–44.
- Glaessgen A, Jonmarker S, Lindberg A, Nilsson B, Lewensohn R *et al*. Heat shock proteins 27, 60 and 70 as prognostic markers of prostate cancer. *Apmis* 2008; **116**: 888–95.
- Miyake H, Muramaki M, Kurahashi T, Takenaka A, Fujisawa M. Expression of potential molecular markers in prostate cancer: correlation with clinicopathological outcomes in patients undergoing radical prostatectomy. *Urol Oncol* 2010; **28**: 145–51.
- Grotendorst GR, Lau LF, Perbal B. CCN proteins are distinct from and should not be considered members of the insulin-like growth factor-binding protein superfamily. *Endocrinology* 2000; **141**: 2254–6.
- Jenkins PJ, Bustin SA. Evidence for a link between IGF-I and cancer. *Eur J Endocrinol/ Eur Federat Endocrine Soc* 2004; **151** (Suppl 1): S17–22.
- Roddam AW, Allen NE, Appleby P, Key TJ, Ferrucci L *et al*. Insulin-like growth factors, their binding proteins, and prostate cancer risk: analysis of individual patient data from 12 prospective studies. *Ann Intern Med* 2008; **149**: 461–71, W83–8.
- Degraff DJ, Malik M, Chen Q, Miyako K, Rejto L *et al*. Hormonal regulation of IGFBP-2 proteolysis is attenuated with progression to androgen insensitivity in the LNCaP progression model. *J Cellular Physiol* 2007; **213**: 261–8.
- Uzoh CC, Holly JM, Biernacka KM, Persad RA, Bahl A *et al*. Insulin-like growth factor-binding protein-2 promotes prostate cancer cell growth via IGF-dependent or -independent mechanisms and reduces the efficacy of docetaxel. *Br J Cancer* **104**: 1587–93.
- Geier R, Adler S, Rashid G, Klein A. The synthetic estrogen diethylstilbestrol (DES) inhibits the telomerase activity and gene expression of prostate cancer cells. *Prostate* 2010; **70**: 1307–12.
- Cavaliere E, Frenkel K, Liehr JG, Rogan E, Roy D. Estrogens as endogenous genotoxic agents—DNA adducts and mutations. *J Natl Cancer Inst Monogr* 2000; (27): 75–93.